Rev. Roum. Sci. Techn.– Électrotechn. et Énerg.
Vol. **70**, *3*, pp. 427–432, Bucarest, 2025

USEFUL ASSUMPTION FOR SIMPLIFIED NUMERICAL ANALYSIS OF TRANSCRANIAL MAGNETIC STIMULATION

CHRIS-MARIA CIOCĂZANU[1], DENISA-ELENA NIŢESCU[2], MIHAELA MOREGA[3]

Keywords: Transcranial magnetic stimulation (TMS); Inductor current; Numerical analysis; Finite element method (FEM).

Magnetic stimulation is a bioelectromagnetic effect of exposing the human body to a time-varying magnetic field; excitable tissues (nerves, muscles, sensory organs) can be activated by the electric field (or associated electric current) generated by electromagnetic induction. The biological effects of stimulation have medical applications in a dynamic class of neuromodulation techniques, such as transcranial magnetic stimulation. However, hazardous human exposure to low-frequency, high-amplitude magnetic fields may also be associated with an increased incidence of health risks, as observed in specific occupational exposure scenarios. This study presents some typical issues related to the numerical simulation of electromagnetic field problems in this class (formulation, data, methods, implementation, accuracy), provides specific quantitative estimates (postprocessing of electromagnetic solutions), and illustrates the practical possibility of reducing the consumption of computational resources by adopting a simplified problem description that replaces a transient analysis with a time-harmonic analysis.

1. INTRODUCTION

As a commonly used expression in medical applications, "magnetic stimulation" is an abbreviation for "activation of excitable tissues by electrical stimuli generated by electromagnetic induction" (inductive coupling), an alternative procedure to the traditional "electrical stimulation" by direct electrical contact through electrodes (resistive coupling).

Electromagnetic induction is utilized in various medical technologies, ranging from nerve or muscle stimulation to hyperthermia. However, it also highlights potential health risks associated with human exposure to variable magnetic fields, particularly in hazardous work environments. The technical approach to bioelectromagnetic interactions is based on theory (understanding of physical principles), equipment (design and manufacture of electrical devices that represent the primary sources of magnetic fields), and analysis and evaluation methods derived from electrical engineering (numerical simulation and electromagnetic field measurements).

The analysis conducted in this study refers to transcranial magnetic stimulation (TMS), a non-invasive neurotechnology that generates short electrical stimuli within the cortex to activate neuronal structures. The pulsed stimuli are triggered by electromagnetic induction as follows: high amplitude pulsed currents feed an applicator (electromagnetic emitter), externally placed on the scalp; the coil is inductively coupled with the underlying tissue (electromagnetic receiver), notably with the conductive and excitable neuronal layers in the cortex, where induced currents act as electrical stimuli for the membranes of nearby axons and lead to local changes in transmembrane voltage. Depending on the polarity of the stimulus, the membrane electrical response is different - transmembrane voltage could either (1) increase above its resting value and the membrane could eventually depolarize (activate) if the stimulus exceeds a certain threshold level, or (2) decrease to more negative values toward a hyperpolarization (inhibition) membrane condition [1]. Membrane depolarization means the generation of transmembrane voltage impulses, in the form of action potentials; this type of electrical activation of the neuronal membrane (specifically axonal) is harnessed in neuromodulation interventions. The effectiveness of induced electrical stimuli in magnetic stimulation depends on their magnitude and polarity, which are conditioned by the magnitude and polarity of the inductor's magnetic flux and by its rate of change [2–4].

The basic design of most commercial TMS devices originates in the electrical schemes patented by Anthony Barker and his team. In 1985, after several years of research, they successfully demonstrated the scientific benefits of cortical stimulation performed through electromagnetic induction and its potential medical applications [5] at the Royal Hospital in Sheffield, UK. The experimenters are credited as inventors of the TMS medical technique, and their demonstration triggered an avalanche of research works on the procedure. Soon after, Magstim Ltd. initiated the fabrication of magnetic stimulation devices under an exclusive license with the University of Sheffield, starting with the model released in 1986, which featured a single circular coil (like the original design used by the inventors). During the following decades, the company developed and continually improved its entire Magstim 200[2] series [6], offering today truly advanced neuromodulation technology devices that are widely appreciated in clinical interventions [7]. Other companies soon began producing TMS equipment, while also supporting research; starting in 2008, the FDA (Food and Drug Administration of the USA) began issuing approvals for various TMS-type medical therapies, enabling their clinical application [4].

The efficiency of the TMS technique relies on the precision of localization and the proper settings of the stimuli. Therefore, TMS devices and protocols for specific therapies are being adapted and refined for the research and treatment of various neuropsychiatric conditions. The evolution of neuromodulation techniques is aligned with the need for personalized therapeutic settings, and therapists are continually faced with the need to design and optimize their instruments. In the last decades, various types of applicators and operating protocols have been researched. The specialized literature presents comparative studies on their performance regarding the optimal localization of the stimulus within the brain, which can be expressed in indicators such as focus, penetration depth, and minimizing side effects (such as heating, stimulation at the surface, or in neighboring regions) [8–10]. This is why the study presented here aims to show and validate shortcut approaches for finding reliable operating parameters of TMS through fast and economical numerical simulation; it might not be necessary to perform repetitive laborious computation (*i.e.*,

[1,2,3] Doctoral School of Electrical Engineering, Romania, National University of Science and Technology Politehnica Bucharest, Romania.
E-mails: chris.ciocazanu@upb.ro, denisa.nitescu@upb.ro, mihaela.morega@upb.ro

DOI: 10.59277/RRST-EE.2025.70.3.23

accurate simulation in realistic conditions) for results aimed to simply compare performances among similar designs. The focus here is on the inductor current waveform and the choices between transient and harmonic analysis modes adopted for the electromagnetic problem.

Quantitative data used through this study to illustrate and support the examples accompanying theory are inspired by the products of the commercial TMS Magstim 200² series [7]. Simple circular coil applicators powered by monophasic pulsed currents were used, considering that the simplest design fits well enough for validating the concepts and analysis methods addressed in this study.

2. WAVEFORM OF THE INDUCTOR CURRENT

Pulsed waveforms, either mono- or biphasic, are the classic choice in TMS for the current powering the applicator, motivated both by the ease of current generation and the effectiveness of the triggered stimulus for neuromodulation purposes [1, 10].

2.1 ELECTRICAL CIRCUIT AND BASIC MONOPHASIC PULSE

Fig. 1 shows the main components of an electrical circuit for the generation of monophasic current pulses, preferred in cortical stimulation [6]. Basically, the pulsed current arises from the fast discharge of a capacitor *C*, on the *R-L* circuit represented by the applicator (induction coil) and an additional resistance R_s used for the adjustment of electrical parameters. The capacitor is previously charged up to a pre-defined voltage, and its fast discharge is controlled via a switching device, which could be a simple commutator, or an electronic rectifier (active switching device), able to modulate the high intensity current pulse, especially the rising phase, important in controlling the stimulus magnitude. The current induced in the target tissue (*i.e.* the stimulus) is proportional to the rising slope of the current through the applicator; Maxwell's theory (the law of the magnetic circuit and the law of induction) explains the determination of the induced current by the magnetic field of the inductor, respectively by its source, the coil current *i(t)*.

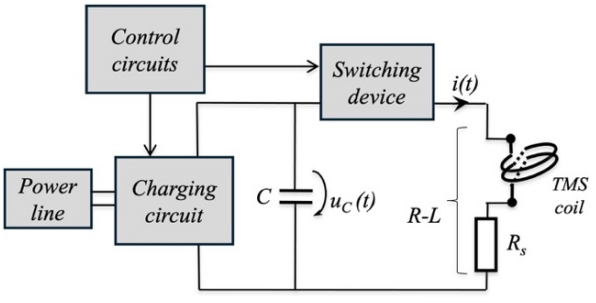

Fig. 1 – Basic electrical circuit for feeding the TMS applicator with monophasic current pulses. (after [10])

A comprehensive review of the literature and an analysis of different current control solutions through electronic switching devices, as well as their performances (mainly derived from the need to switch high current) are presented in [10]. The dynamic regime triggered by an ideal discharge of *C* is generally described by the classical expressions of voltage and current (canonical solutions of the characteristic equation of the circuit)

$$u_C(t) = U_0 e^{-\propto t}(\mathrm{ch}\omega t + \frac{\propto}{\omega}\mathrm{sh}\omega t), \qquad (1)$$

$$i(t) = \frac{U_0}{\omega L} e^{-\propto t}\mathrm{sh}\omega t, \qquad (2)$$

with $U_0 = u_C(t)_{|t=0}$ the initial discharge voltage, $\propto = R/2L$ the attenuation constant of the circuit and $\omega = \sqrt{\left(\frac{R}{2L}\right)^2 - \frac{1}{LC}}$ the angular frequency of oscillation. A typical monophasic current pulse results as *the critically damped response* by properly sizing the circuit elements under the condition

$$R = 2\sqrt{L/C}\,. \qquad (3)$$

The coil current *i(t)* becomes

$$i(t) = \frac{U_0}{L}\, t\, e^{-\propto t}, \qquad (4)$$

with its maximum $I_m = \frac{U_0}{L}\frac{1}{\propto}e^{-1}$ for the moment $t_m = \frac{1}{\propto}$; its general waveform (Fig. 2) is adjustable by setting adequate values for the voltage U_0 and for the circuit elements *R*, *L*, *C*.

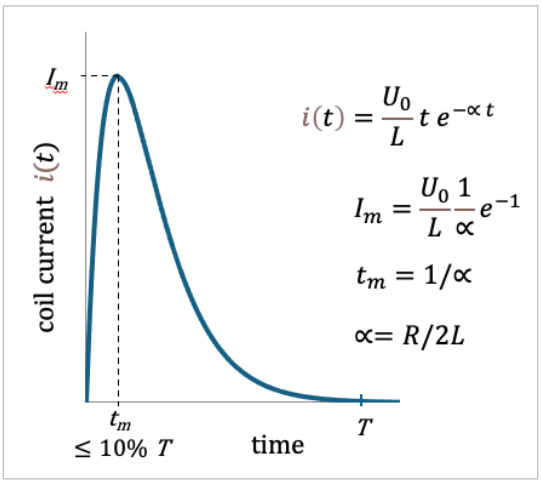

Fig. 2 – Common waveform of the monophasic pulse current through the TMS coil, representing the critically damped response of the circuit in Fig. 1.

One monophasic pulse for TMS is usually generated at very high amplitude, in the range of (5 … 10) kA, with a duration *T* of cca. 1 ms, a steep initial rise in the order of 10^8 kA/s and a rise-time of (50 … 100) μs up to its peak. For such a result, appropriate ranges for the circuit data are: $U_0 \approx (3 \ldots 8)$ kV; $L \approx (12 \ldots 25)$ μH; $R \approx (0.3 \ldots 0.5)$ Ω; $C \approx (200 \ldots 700)$ μF [11–13]. The equivalent resistance of the circuit includes the resistance of the coil R_{coil} and the additional resistance R_s. Design calculations show that $R_{coil} << R_s$, which emphasizes the importance of R_s as a useful means of compensating for dispersions of other parameters. At the same time, an increase in R_{coil} in reaction to the fluctuating magnetic field is most likely insignificant.

When a certain type of applicator is designed, the inductance *L* is mainly fixed by its structure (number of turns, shape, size of the conductor and configuration). For example, common values of some characteristics could be seen in Table 1 for three simple circular-coil models of the series Magstim 200² [6].

The capacitance *C* and the initial voltage U_0 might be conveniently chosen, while the resistance *R* needs to be adjusted through its component R_s (Fig. 1) such as to ensure the critically damped waveform (see the condition introduced above by eq. (3)).

Table 1
Technical data for a selection of Magstim 200² series circular coils [6].

Coil type → ↓ Characteristic	P/N 9999, 50mm	P/N 9762, 70mm	P/N 3192/3, 90mm
Coil Diameters D_{int} / D_{ext} [mm]	25 / 77	40 / 94	66 / 123
Number of turns N	18	15	14
Inductance L [10^{-6} H]	13.5	16	23.5
Peak Magnetic Flux Density [T]	3.6	2.6	2.0

2.2 CIRCUIT DESIGN AND WAVEFORM CHARACTERISTICS

An example of circuit design is shown below. Let's consider having an average coil with the inductance $L = 16$ μH; the objective is to get a standard waveform of the current pulse with the peak of I_m = 8 kA at t_m = 0.1 ms, as adopted also by manufacturers of stimulation equipment [6]. According to the above equations, the attenuation constant should be $\propto = \frac{1}{t_m} = 10^4$ s^{-1}, the resistance is adjusted to $R = 2L \propto = 0.32\ \Omega$ and the required capacitance should be $C = \frac{4L}{R^2} = 625$ μF; it needs to be charged by a voltage $U_0 = 3.48$ kV. This circuit design solution leads to the current waveform drawn in Fig. 3 with a solid dark line.

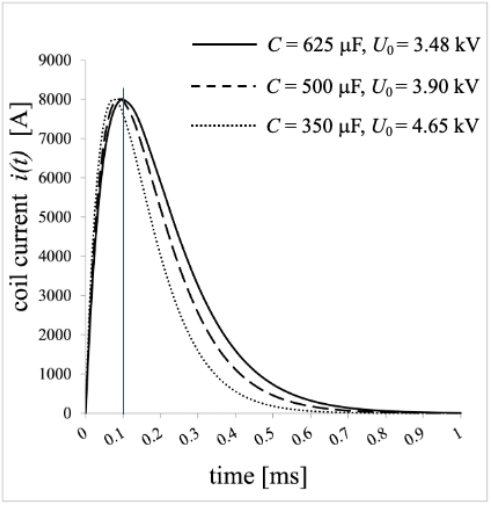

Fig. 3 – Pulse current waveforms for different circuit parameters.

Other useful results, presented below for the same coil with the inductance $L = 16$ μH are obtained by a parametric study showing the influence of optional circuit data on the waveform of the coil current. Fig. 3 shows modified waveforms of the pulse due to different values of C; the parameters R and U_0 are adjusted to maintain the same required value of I_m = 8 kA. With decreasing capacitance, the pulse rise-time t_m decreases slightly, which means that the initial slope of the current waveform dI/dt (*i.e.* di/dt at t = 0) increases, which makes the actual stimulus larger. These variations are not linear, so it is interesting to see in Table 2 the values of the main quantities analyzed here and to understand the determinations between them.

As the previous example shows, simple adjustments of circuit parameters are efficient, either to generate a desired waveform of the coil current (and consequently of the stimulus), or to compensate design approximations; the actual coil characteristics (values of R_{coil} or L) might be slightly different from their calculated values. Additionally, under operating conditions, R_{coil} and L could have slight dispersions (difficult to predict accurately from design) because of the varying magnetic field, such as the skin effect in conductors, or inductive coupling between the coil and the tissue.

Table 2
Useful values of the main circuit parameters and their influence on the pulse waveform.

parameters of the electrical circuit					parameters of the 8 kA pulse	
L [μH]	C [μF]	R [mΩ]	α [s^{-1}]	U_0 [kV]	t_m [μs]	dI/dt [A/s]
16	625	320	10000	3.48	100	$2.18 \cdot 10^8$
16	500	358	11200	3.90	89	$2.44 \cdot 10^8$
16	350	428	13400	4.65	75	$2.91 \cdot 10^8$

2.3 TRANSIENT VERSUS TIME-HARMONIC ANALYSIS TYPE

Between transient (time domain) and time-harmonic (frequency domain) analysis there is a huge difference in a numerical approach, in terms of the required computational resources, as also observed in [12]. The transient mode follows the time variation of the quantities and describes the system at each time step of the process by solving the differential equations at every time step, while the time-harmonic analysis is based on the complex representation of the quantities and the solution is applied only once, to a system of algebraic equations. This fundamental economic advantage is usually capitalized by researchers and most TMS simulation studies assume the harmonic mode. However, the choice of a particular nominal frequency is not fully motivated, although, as this study further shows, it is a parameter that significantly affects the results; usually, authors opt for the so-called *dominant spectral component* associated with the impulse, which is of the order of kHz (*e.g.* 3 kHz was assumed in [14], 10 kHz in [15], 5 kHz in [8]). Decomposing the pulse waveform into harmonic Fourier components could be another approach, and Barchanski explores it in [12] with considerable computational effort.

Here, a comparison of the transient and time-harmonic analysis modes is made in terms of accuracy and computer resources, with an original selection of the nominal frequency. Let's first introduce the two waveforms considered for the coil current – the classic monophasic pulse versus a sine wave, following as closely as possible the rising phase of the respective pulse.

Figure 4 presents the starting time interval of the conventional short pulse (a) (data on the first line of Table 2), versus two sine waveforms (b) and (c), $i_s(t) = I_m \sin 2\pi f t$, with the same peak value as the pulse $I_m = 8$ kA. The sine-waves frequencies differ. Sinewave (b) has the frequency $f' = \frac{1}{4t_m} = 2.5$ kHz and shows the best fit to the pulse for the rise time $t_m = 0.1$ ms, but its initial slope is only dI/d$t \approx 1.26 \cdot 10^8$ A/s. On the other hand, sine-wave (c) has the frequency $f'' = 4.35$ kHz and shows the best fit to the pulse for the initial slope dI/d$t \approx 2.18 \cdot 10^8$ A/s, but has a corresponding rise time $t_m \approx 0.057$ ms.

TMS analysis is reduced here to only a short interval, right at the beginning of the pulse, when the coil current features (especially its time derivative) really matter for the purpose of stimulation; no need to study the TMS process over a long period of time, because the quantity of interest – the stimulus (electric field strength or current density induced within the

target tissue) – is most likely to exceed a strength-duration threshold from its very first moments.

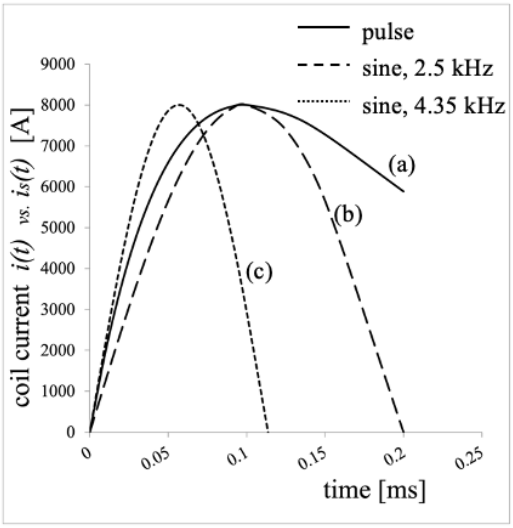

Fig. 4 – Waveforms of the coil current, all with I_m = 8 kA:
(a) pulse given by eq. (4), with t_m = 0.1 ms, dI/dt = 2.18·10^{8}A/s;
(b) sinewave with f ‘ = 2.5 kHz, t_m = 0.1 ms, dI/dt = 1.26·10^{8}A/s;
(c) sinewave with f “ = 4.35 kHz, t_m = 0.057 ms, dI/dt = 2.18 ·10^{8}A/s.

Stimulus thresholds vary depending on the target type and subject sensitivity; the literature provides conjectural and approximate limits, such as 6 A/m² at 2.44 kHz and 2.5 A/m² at 50 Hz, for stimulation of the upper limb motor cortex area [11]. These values are approximately two orders of magnitude above the safety levels (*i.e.*, avoiding electrostimulation) documented in the IEEE C95.1-2019 standard for human protection from magnetic fields in the low-frequency range [16]. Following research results, manufacturers of TMS equipment consider almost as a benchmark of efficiency a short rise time in the range of (0.05 … 0.1) ms and an initial slope of the order of 10^8 A/s for the coil current waveform [6]; these reference values are also adopted by [12] and [13], while [17] establishes a stimulation efficiency threshold on the induced electric field strength of 100 V/m, regardless duration.

2. NUMERICAL MODEL

Three models were proposed above to emulate the waveform of the current through the coil (Fig. 4), particularly during its starting sequence, which is considered significant for triggering an efficient stimulus. We explore here the possibility of addressing the *quasi-static magnetic* operation mode in TMS through the economical *time-harmonic analysis* (associated with sinewaves), as an alternative to *transient analysis* (associated with the pulsed waveform of the inductor current).

Since the comparison of analysis types does not depend on the applicator characteristics (which, in fact, are the same for both types of analyses), a minimalistic configuration is adopted here, *i.e.,* the simple circular coil in a symmetrical position above the vertex, as shown in Fig. 5, as described in extenso by [4].

Head structure consists of three types of tissues (skull, brain, eyes), with electrical conductivities specific to the frequency spectrum involved in TMS, the kHz range (0.02 S/m, 0.1 S/m, and 1.5 S/m, respectively). The domain is bounded by a spherical surface that brings no constraints to the magnetic field distribution. If the domain has symmetry with respect to the sagittal plane, only half of the entire geometry is required for the calculation. However, maintaining the entire geometry here has advantages in validating the results and the model is ready for further studies involving different (asymmetric) applicator positions and configurations.

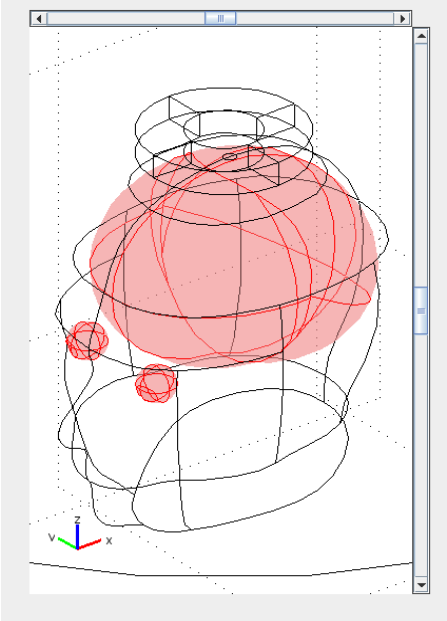

Fig. 5 – Numerical model of the head and TMS applicator. The simple circular coil is placed symmetrically above the vertex of the head, its base stands on the xOy, z=0 Cartesian coordinates plane, while the circular coil’s axis coincides with the Oz axis.

The coil is part of the capacitor discharge circuit (Fig. 1), and the main circuit parameters are listed on the first line of Table 2 in the case of the standard monophasic pulse. Fig. 4 shows data on the coil current waveforms, analyzed and compared in this study: pulse waveform (a) for the transient analysis, sinusoidal waveforms (b) and (c) for the time-harmonic analyses.

The electromagnetic analysis is performed here with the FEM numerical method in COMSOL Multiphysics, the AC/DC module for quasi-static magnetic operation mode (transient versus time-harmonic analysis).

3. RESULTS

This study compares the numerical results obtained by simulation with those from 3D numerical models for the coil current waveforms shown in Fig. 4. A time-domain electromagnetic analysis solves the TMS problem for the pulse current (a). In contrast, for the time-harmonic waves (b) and (c), the studies are performed in the frequency domain. To begin with, the magnetic field spectrum is shown in Fig. 6 for the peak inductor current through the coil (waveform (a), $i = I_m$ = 8 kA, t = 0.1 ms). It should be noted that identical spectra are obtained for the two sinusoidal waveforms (b) and (c) for the peak value of 8 kA (although these are not shown here).

Distributions of the magnetic field and induced current inside the head, particularly in specific cortical target regions, are of interest within the TMS procedure. Therefore, a more precise comparison between the results recorded in the three cases (currents of form (a), (b), and (c), shown in Fig. 4) is presented below.

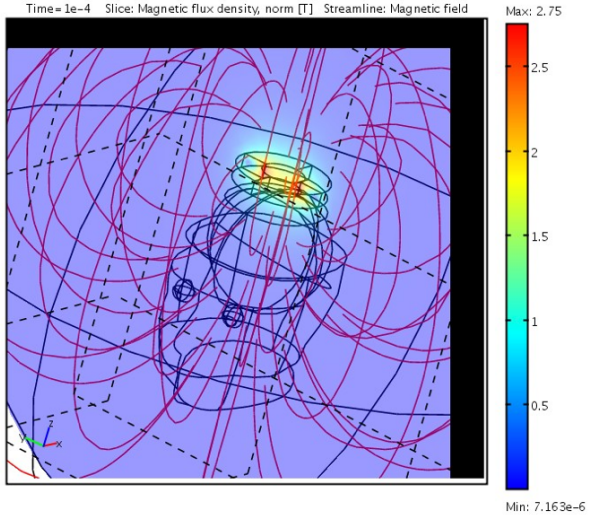

Fig. 6 – Color map of the magnetic field density in the frontal plane of the head (color scale in [T]) and magnetic field spectrum (field lines in red color), for the time domain analysis (pulse current); the results correspond to $i(t) = I_m = 8$ kA and $t = t_m = 0.1$ ms.

Ensuring similar conditions of assessment, the distributions of these electromagnetic quantities are compared next; the graphs shown in Fig. 7 support this task. Relevant electromagnetic quantities are acquired along two observation lines crossing the head, parallel to the horizontal y-axis, at coordinates z = -0.02 m (for the red curves) and z = -0.03 m (for the blue curves); the observation lines are included here in cross-sectional planes that cross the head through the brain, not through the eyes. The line pattern is associated with the models described above, exactly as for the current waveforms in Fig. 4: the solid line represents the time domain analysis (pulse waveform). In contrast, for frequency domain analysis (sinewaves), the dotted line is used for 4.35 kHz and the dashed line for 2.5 kHz accordingly. Fig. 7.a presents the magnetic field density, where all three models show identical results (plain, dotted, and dashed lines are superposed), which is normal because the magnetic flux density is computed here for the same peak value of the current (8 kA) regardless of its waveform. Figure 7.b illustrates different results that are compared; the time domain analysis is best equated with the frequency domain analysis at 4.35 kHz, *i.e.* the values on the solid line curves are very close to those on dotted line curves (relative errors below 5 %), while the dashed line curves show considerably different values from the homologous ones.

The comparison between time and frequency-domain approaches and the best choice for the operating frequency value are also supported by comparing several global electromagnetic quantities, presented in Table 3. It is again obvious that the time-domain analysis could be conveniently replaced by the frequency-domain analysis, provided the appropriate frequency is chosen (in the context discussed here for TMS, the 4.35 kHz sinusoid emulates very well the pulse represented by the solid line in Fig. 3 and Fig. 4).

4. CONCLUSIONS

Despite the huge efforts devoted in the last decades to the detailed anatomical formulation and precise analysis of TMS numerical problems [18], the profit comes mainly from theoretical progress (advance of computational methods and models), while the clinical benefit is still based on experimental, quasi-empirical research [7].

Table 3

Comparison of several global quantities computed in the subdomain "brain".

type of analysis →	time domain analysis	frequency domain analysis	
↓ electromagnetic quantity related to the brain	pulse	sine (4.35 kHz)	sine (2.5 kHz)
absorbed power (total) [W]	2.34	2.38	0.785
absorbed power density (averaged) [W/m^3]	1047	1062	351
induced current density (averaged) [A/m^2]	75.48	76.06	43.7
induced electric field strength (averaged) [V/m]	7.55	7.61	4.37

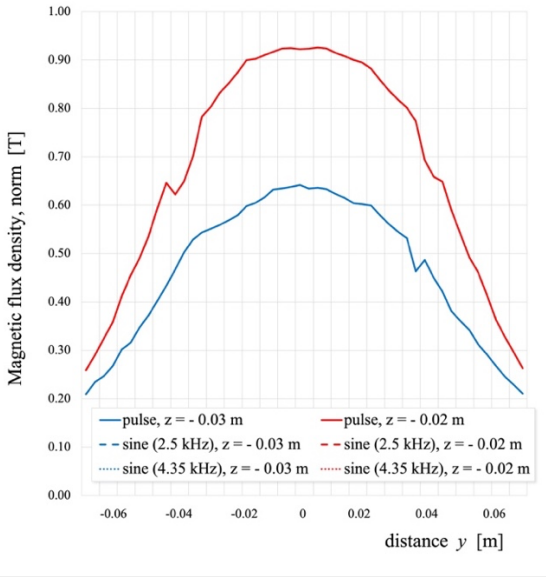

a. Magnetic flux density – peak values corresponding to peaks of coil currents, as shown in Fig. 4.

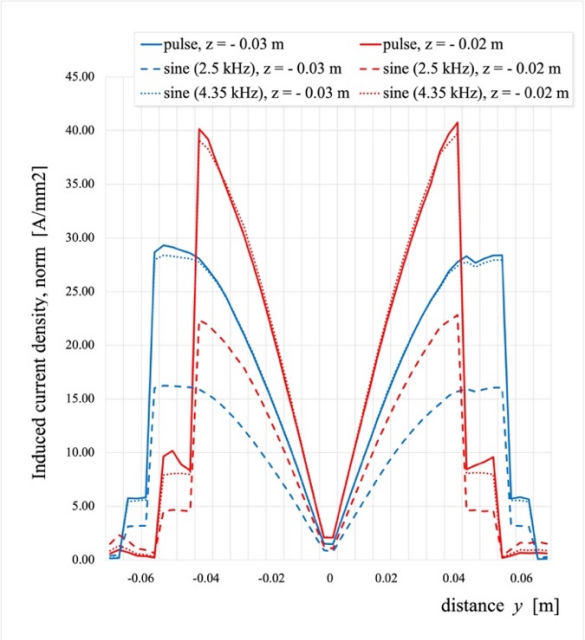

b. Induced current density – peak values corresponding to maximum slope of coil currents shown in Fig. 4.

Fig. 7 – Distributions of specific TMS quantities along observation lines following the direction of the y-axis of the coordinate system, at z = -0.02 m (red) and z = -0.03 m (blue).

Despite the huge efforts devoted to the detailed anatomical formulation and precise analysis of TMS numerical problems over the last few decades [18], the benefits mainly stem from theoretical progress (advances in computational methods and models), while the clinical benefit remains based on experimental, quasi-empirical research [7]. Medical aspects such as dosimetry correlations between technical parameters (configuration and position of coils, amplitude and waveform of coil currents, distances, etc.) and therapeutic effects are still affected by many unknowns. Even advanced models do not consider all significant phenomena (endogenous physiological background, subtle bioelectromagnetic interactions or side effects) and are not able to provide predictions, accurate and reliable enough for clinical implementation, as is the case in many other branches of interventional medicine assisted by modern technologies, for example those illustrated by [19] or by [20].

Although the physics and numerical simulation of TMS procedures are typical matters of applied electromagnetism, and modern image processing techniques could help with precise anatomical localization, the biological process of neuromodulation with electrical stimuli still has many subtle aspects, beyond the technical approach and prediction. However, numerical simulation proves its usefulness for technical operations such as computer-aided design of TMS equipment and their optimization, exploring the correspondence between coil position and target location, or educating therapists and technicians on the flow of phenomena (mainly electromagnetic interactions) based on balanced quantitative approximations.

We have explored here the possibility of replacing the "time-domain approach" (*i.e.*, transient analysis associated with the pulsed waveform of the inductor current) with a "frequency-domain approach" (*i.e.*, time-harmonic analysis based on a complex number representation, related to sinusoidal signals). The good agreement of the results obtained by the two methods is conditioned by a suitable selection of the operating frequency, and the selection method is described in this study. Based on our promising results, we recommend the simplified approach of TMS simulation in the frequency domain as a convenient method for performing rapid analyses on various data sets and case studies, while saving considerable computational resources.

ACKNOWLEDGMENT

The authors would like to thank the University Politehnica Bucharest for full access to the computing resources within the Laboratory of Electrical Engineering in Medicine, Faculty of Electrical Engineering, and for the support provided by the Doctoral School of Electrical Engineering.

CREDIT AUTHORSHIP CONTRIBUTION

Mihaela Morega: investigation (model definition, computation, postprocessing)
Chris-Maria Ciocăzanu: investigation (model validation, postprocessing, graphics)
Denisa-Elena Nițescu: conceptualization, methodology, writing

Received on 8 July 2025

REFERENCES

1. S. Ueno, M. Sekino, *Biomagnetics. Principles and Applications of Biomagnetic Stimulation and Imaging (Chapters 2 and 3 on Biomagnetic Stimulation)*, CRC Press, Taylor&Francis Group (2016).
2. P.M. Rossini et al., *Non-invasive electrical and magnetic stimulation of the brain, spinal cord, roots and peripheral nerves: Basic principles and procedures for routine clinical and research application*, Report from an IFCN Committee, Clinical Neurophysiology, **89**, *6*, (2015).
3. A.M. Morega, M. Morega, A.A. Dobre, *Computational Modeling in Biomedical Engineering and Medical Physics (Chapter 7 - Magnetic stimulation therapy),* Academic Press, Elsevier Inc., pp. 217-245 (2021).
4. C.M. Ciocăzanu, N.S. Stanciu, M. Morega, *An Electrical Engineering Perspective on Neuromodulation – Characteristics of the Magnetic Stimulation Procedure*, U.P.B. Sci. Bull., Series C, **86**, *4*, pp. 349–366 (2024).
5. A.T. Barker, R. Jalinous, I.L. Freeston, *Non-Invasive Magnetic Stimulation of Human Motor Cortex,* The Lancet. **325**, *8437*, pp. 1106–1107 (1985).
6. C. Hovey, R. Jalinous, *The Guide to Magnetic Stimulation*, © The Magstim Company Ltd. (2006).
7. ***Magstim® Inc., *Pioneers in Neurotechnology. MAGSTIM TMS Catalog* The Magstim® Company Ltd. (2024).
8. Z.D. Deng, S.H. Lisanby, A.V. Peterchev, *Electric field depth-focality tradeoff in transcranial magnetic stimulation: Simulation comparison of 50 coil designs*, Brain Stimul. **6**, pp. 1–13 (2013).
9. V. Guadagnin, M. Parazzini, S. Fiocchi, I. Liorni, P. Ravazzani, *Deep Transcranial Magnetic Stimulation: Modeling of Different Coil Configurations*, IEEE Trans. Biomed. Eng., **63**, *7*, pp. 1543–1550 (2016).
10. M.I. Gutierrez, et al., *Devices and Technology in Transcranial Magnetic Stimulation: A Systematic Review*, Brain Sci., **12**, *9*, art. no. 1218 (2022).
11. T. Kowalski, J. Silny, H. Buchner, *Current density threshold for the stimulation of neurons in the motor cortex area*, Bioelectromagnetics **23**, *6*, pp. 421–428 (2002).
12. A. Barchanski, *Simulations of Low-Frequency Electromagnetic Fields in the Human Body*, PhD Thesis, TU Darmstadt (2007).
13. S. Ueno, *New Horizons in Electromagnetics in Medicine and Biology*, Radio Science, **56**, *4*, 17 pages (2021).
14. D. Rafiroiu, S. Vlad, L. Cret, R. Ciupa, *3D Modeling of the Induced Electric Field of Transcranial Magnetic Stimulation*, IFMBE Proc., **26**, pp. 333–338 (2009).
15. N.J. Tachas, K.G. Efthimiadis, T. Samaras, *The Effect of Coil Modeling on the Predicted Induced Electric Field Distribution During TMS*, IEEE Transactions on Magnetics, **49**, *3*, pp. 1096–1100 (2013).
16. ***IEEE Std C95.1-2019 for *Safety Levels with Respect to Human Exposure to Electric, Magnetic, and Electromagnetic Fields, 0 Hz to 300 GHz*, Annex B.2 *Rationale for limits based on electrostimulation*, Copyright © 2019 IEEE.
17. M. Lu, S. Ueno, *Computational Study Toward Deep Transcranial Magnetic Stimulation Using Coaxial Circular Coils,* IEEE Transactions on Biomedical Engineering, **62**, *12*, pp. 2911–2919 (2015).
18. E. Salkim, T. Abut, *Human Head Transcranial Magnetic Stimulation using Finite Element Method*, Kocaeli Journal of Science and Engineering, **7**, *1*, pp. 62–70 (2024).
19. A. Ramaiah, P.D. Balasubramanian, A. Appathurai, M. Narayanaperumal, *Detection of Parkinson's disease via Clifford gradient-based recurrent neural network using multi-dimensional data*, Rev. Roum. Sci. Tech. – Électrotechn. et Énerg., **69**, *1*, pp.103–108 (2024).
20. L.E. Dorobanțu, *Biomedical Signal Processing in Cognitive Research: Brain Fingerprinting and Polygraph Testing*, Rev. Roum. Sci. Techn.–Électrotechn. et Énerg., **70**, *2*, pp. 263–268 (2025).